JOURNAL OF MATERIALS SCIENCE **38** (2003) 391 – 400

Review
Review of electrooptic and ferroelectric properties of barium sodium niobate single crystals

K. SAMBASIVA RAO
Centre for Piezoelectric Transducer Materials, Department of Physics, Andhra University, Visakhpatnam 530 003, India
E-mail: Konapala@Satyam.net.in

KI HYUN YOON
Research Institute of Advanced Materials, Yonsei University, Seoul, 120–749, South Korea

Barium Sodium Niobate (BNN) belongs to tungsten bronze type Ferroelectric material. The non linear coefficients of BNN are twice that of $LiNbO_3$. Large single crystal of BNN is useful in frequency doubling applications because its conversion efficiency and resistance to optical damage are superior to $LiNbO_3$. Present review describes the preparative details, sturcture, ferroelectric and electro optic properties of BNN.

1. Introduction

Barium Sodium Niobate, ($Ba_2NaNb_5O_{15}$) (BNN) is a ferroelectric crystal with filled Tungsten Bronze structure. It has been studied extensively over the past thirty five years. BNN possess a sequence of four or more phase transitions that involve ferroelectric, ferroelastic, and incommensurate (IN) phenomena. It has an excellent electro-optic and nonlinear optical properties. It has been used in frequency doubling applications because of its conversion efficiency and resistance to optical damage are superior to those of other known materials such as $LiNbO_3$ (LN). The useful nonlinear coefficients of BNN are twice that of LN. The only limitation which impairs the device application of this material is the occurance of micro-twinning associated with the tetragonal to orthorhombic phase transformation at 260°C. Despite micro-twinning associated with BNN, it has been used as (1) a second harmonic crystal within a laser cavity acts as an output coupler in a manner analogous to a transmitting mirror in a normal laser. (2) One can have a set of resonators with working frequencies in the range of 200–400 MHz has been made up of acoustic super lattice of BNN crystal. (3) Static photorefractive gratings have been recorded by a running inteferance pattern in the ferroelectric crystal, BNN with an external applied ac field. (4) BNN can be used to measure order paramter estimation by measuring thermal lens effect. In BNN dn_c/dt is approximately $+3 \times 10^{-3}$ K^{-1} at T_c and produces a sharp positive focal lenth lens.

In view of the technological relevance [1–5] of the material, BNN the present paper reviews the structure, synthesis, ferroelectirc, and electro-opotic properties of BNN.

2. Structure

Tungsten bronze compounds have structures that are related to K_xWO_3, Na_xWO_3 can be represented by the chemical formulae $(A_1)_4$ $(A_2)_2$ C_4 B_{10} O_{30} and $(A_1)_4$ $(A_2)_2$ B_{10} O_{30} in which A_1, A_2, C and B are 15, 12, 9 and 6-fold Oxygen coordinated sites in the crystal. The first formula represents the so called stuffed bronze structure in that all of the A, B and C sites are occupied (e.g., $K_6Li_4Nb_{10}O_{30}$). The second one represents bronzes which are either filled (all A sites being occupied, e.g., $Ba_4Na_2Nb_{10}O_{30}$) or partially filled (5/6 of the A sites occupied, e.g., $Pb_5Nb_{10}O_{30}$). Tungsten bronze materials exhibit either tetragonal or orthorhombic symmetry. The tetragonal tungsten bronze structure has been discussed by Magneli and Blomberg [6] Wadsley [7], Francombe [8] and by Jamieson *et al*. [9].

$Ba_2NaNb_5O_{15}$ has a structure similar to that shown in Fig. 1 above 260°C. The A_1 sites are filled by Na and A_2 sites are filled by Ba. At room temperature the structure is slightly distorted to orthorhombic with lattice parameters a, b and c equal to 17.592 Å, 17.626 Å and 3.995 Å respectively [10]. Since the orthorhombic distortion of BNN is extremely small ($b - a = 0.03$ Å) at room temperature, the difference in the XRD patterns of the two phases below and above the transition is correspondingly difficult to detect. A further demonstration of this lack of resolution is provided by the fact that the room temperature pattern can also be readily indexed in terms of a tetragonal cell [11, 12] with

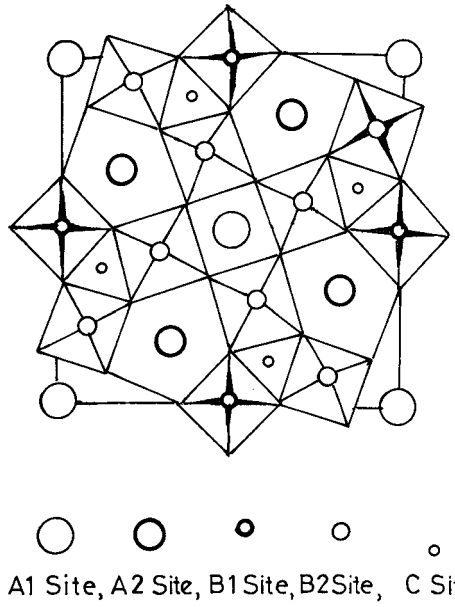

Figure 1 The basic octahedra framework of the tungsten bronze structure looking down the tetragonal *C*-axis.

$a = 12.5$ Å and $c = 4.0$ Å which is known to be the stable structure above 260°C.

3. Synthesis

Scott *et al.* [13] studied the phase equilibria in the $NaNbO_3$–$BaNb_2O_6$ system by DTA and quench techniques and observed that the tungsten bronze phase shows extensive solid solubility from 62 to 83 mole% $BaNb_2O_6$ (Fig. 2). These results were further confirmed by czochralski crystal growth experiments at selected melt compositions in the bronze field. A study of the phase equilibria in the same system was also reported by Carruthers and Grasso [14] whose results indicated an even greater extent of solid solubility in the ternary region of the phase diagram.

BNN crystals grown by czochralski technique, when the melt composition is stoichiometric often exhibit growth striations and tend to crack severely when cooled through ferroelectric transition [15]. Such cracking is shown to be primarily due to lattice distortions associated with the ferroelectric transition. The severity of cracking may be reduced by employing low thermal gradients and shifting the barium niobate content of the melt closure to the congruent melting composition at 69 mole%. Growth striations which cause undesirable changes in refractive index and impair device performance can also be overcome by growing the crystal [16] in the non-stoichiometric congruent melting composition (7.2 Na_2O, 42.2 BaO, 50.6 Nb_2O_5).

Several methods have been proposed to supress microtwinning. Some of these methods are, (1) Cooling the crystal from above the transition temperature under an applied stress, (2) Control of the major growth parameters to minimise growth defects, (3) reducing melt level in a crucible used to contain molten material and (4) formation of a suitable solid solution to lower the transformation temparature from 260°C to room temparature. Detwinning to yield optically homogeneous single crystals has been quite successful.

A comparision of the behaviour of twinned and detwinned crystals of BNN in terms of thermal expansion characterstics has shown that microtwinning in the orthorhombic to tetragonal transition is not a mechanism essential to the transformation, it only occurs in the orthorhombic phase to relieve the large classic strains known to arise in the tetragonal phase on cooling. These measurements further confirm the ferroelectric transition is of a first order change [17]. The growth of uncracked single crystals of BNN for electro-optic and non-linear applications have been developed by Rubin *et al.* [18], Ballman *et al.* [19], Vere *et al.* [20] and Van Uiturt *et al.* [21].

BNN exhibits a large thermal contraction in its C-axis between 350°C and 750°C which causes a serious cracking problem during its crystal growth. Partial substitution of Gd for Ba was found to eliminate the thermal contraction behaviour [22], and polycrystalline BNN of good ferroelectric and dielectric properties for potential electro-optic device applications were synthesised by Tanokura [23].

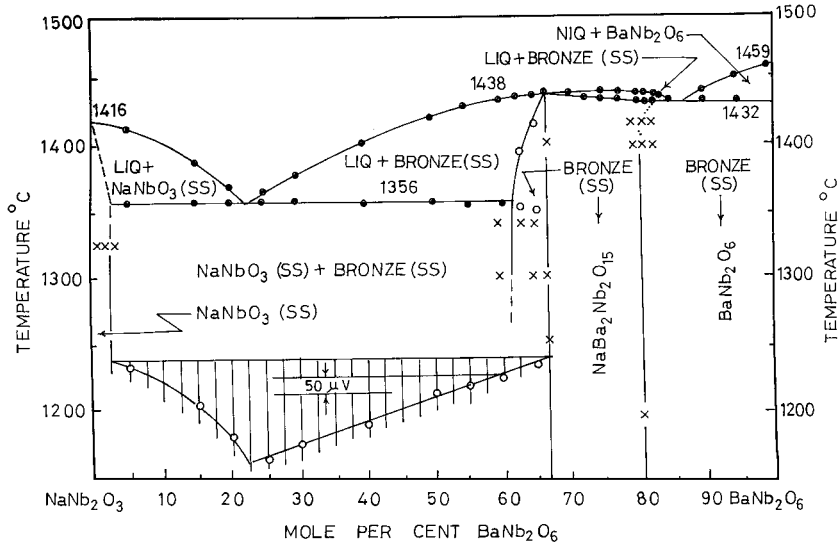

Figure 2 Phase equilibria in the $NaNbO_3$-$BaNb_2O_6$ system. (After [13]).

4. Ferroelectric properties

Ferroelectricity in BNN with a transition at 560°C was established for the first time by Rubin *et al*. [18]. Susequently Burgeat and Toledano [24] reported another transition at 300°C. The first transition is accompanied with a dielectric anomaly while the second corresponds to an elastic anomaly [25]. The ferroelastic transition involved a breakdown of translational symmetry (4 mm → mm 2) as confirmed by X-ray oscillation photographs taken along the *C*-axis [24]. A phenomenological analysis of both transitions is presented by Takuro Ikeda [26]. A microscopic model for mechanism causing ferroelectric phase transition in terms of ferroelectric phonon displacement and dynamic local structural instabilities has been proposed by Reinecke and Ngai [27]. Ferroelectric and ferroelastic properties coexist at room temperature in BNN, but these are not coupled. Toledano [28] demonstrated on the basis of elasticity measurements that spontaneous polarisation is not a possible order parameter of the ferroelastic transition.

Spontaneous polarisation of BNN was measured directly at room temperature by a field reversal method. A comparision of these values with $LiNbO_3$, $LiTaO_3$ and $BaTiO_3$ is given in Table I [29]. A complete set of elastic, piezoelectric and dielectirc constant of BNN at room temperature were reported by Warner *et al*. [30] which are reproduced in Table II. The value K_t equal to 0.57, the coupling factor of BNN was found to be effectively independent of temperature from 0 to 100°C, which makes it a useful material for ultrasonic transducer [30]. Experimental investigation was made of the temperature and frequency dependence of the permitivity and losses in single domain crystals of BNN by Turik *et al*. [31]. It was found that in ferroelectric phase near the curie temperature, considerable discrepancy exists between the measured permitivity and that calculated from the phonon frequencies and this discrepancy was accompanied by high temperature relaxation of permittivity in the range 10^8 Hz. It was found that in BNN crystals, the ferroelectric to paraelectric transition is of relaxation in nature.

TABLE I Room temperature dielectric constant and polarisation data of some oxygen octahedra ferroelectrics (after [29])

Material	T_c (°C)	E_c	E_a	P_s (c/m^2)
Li NbO_3	1195	30	84	0.71
Li TaO_3	610	45	51	0.50
$Ba_2Na\ Nb_5O_{15}$	560	51	242	0.40
Ba TiO_3	120	160	3000	0.25

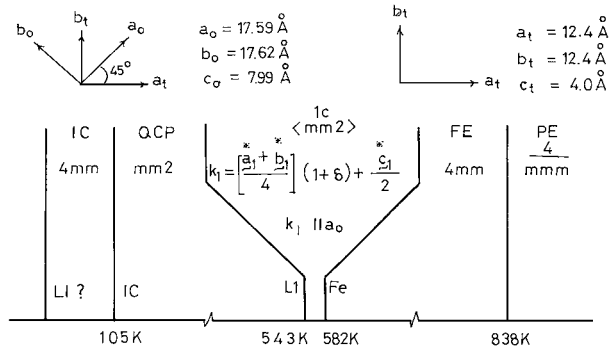

Figure 3 A schematic representation of the different phases in BNN as a function of temperature, as well as the point-group symmetries, lattice constants and relative orientations of the *a* and *b* axis (IC—Incommensurate; QCP—Quasi Commensurate Phase) (after [32]).

Fig. 3. indicates the different phases in BNN as a function of temperature, as well as the point group symmetries, lattice constants and relative orientations of the *a* and *b* axes [32]. Dielectirc and Brillouin spectroscopic measurements on incommensurate BNN from Ca. 15 K to room temperature has been performed by Oliver III *et al*. [33]. They found that the 105 K transition is from $C_c\ m2_1$ to a modulated structure, which appears to be a reentrant phase and also found at atmospheric pressure from 565 K to 582 K. Neutron diffraction studies by the same authors showed the 2_q IC nature of BNN below ∼100 K. The role of pressure in stabilising the different phases in BNN has been discribed by the same authors.

Burns and O'Kane [34] demonstrated that transition temperature variations upto 33°C can be induced in BNN by quenching single crystals from high temperature. This probably accounts for the difference in the reported values of the T_c. Structural behaviour of BNN has been studied in the region of ferroelectric curie point by means of high temperature XRD and DTA. No significant changes in the diffraction pattern have been observed until temperature in the vicinity of T_c are reached; the patterns are consistent with structure retaining tetragonal symmetry through the transition assuming a significantly lower c/a ratio. Thermal expansion measurements proved the transition is of first order in BNN [35].

TABLE II Dielectric, elastic and piezoelectric constants of BNN (after [30])

Dielectric constants		Elastic constants		Piezoelectric constants	
E^S_{11}/E_0	222	C^E_{11}	2.39×10^{11} N/m^2	S^E_{11}	5.30×10^{-12} m^2/N	e_{15}	2.8 C/m^2
E^S_{22}/E_0	22	C^E_{12}	1.04	S^E_{12}	−1.98	e_{24}	3.4
E^S_{33}/E_0	32	C^E_{13}	0.50	S^E_{13}	1.20	e_{31}	−0.4
E^T_{11}/E_0	235	C^E_{22}	2.47	S^E_{22}	5.14	e_{32}	−0.3
E^T_{22}/E_0	247	C^E_{23}	0.52	S^E_{23}	−1.25	e_{33}	4.3
E^T_{33}/E_0	51	C^E_{33}	1.35	S^E_{33}	8.33	d_{15}	4.2×10^{-11} C/N
		C^E_{44}	0.65	S^E_{44}	15.4	d_{24}	5.2
		C^E_{55}	0.66	S^E_{55}	15.1	d_{31}	−0.7
		C^E_{66}	0.76	S^E_{66}	13.2	d_{32}	−0.6
						d_{33}	3.7

TABLE III (After [41–51])

Substituent	Composition	Concentration	T_c (°C)
Chromium	$Ba_{1.9}NaCr_{0.1}Nb_5O_{15}$	0.03 to 0.1	–
Fluorine	$Ba_{2.x}Na_{1+x}Nb_5O_{15-x}F_x$	0.03 to 0.1	–
Gadlonium	$Ba_{1.9}NaGd_{0.1}Nb_5O_{15}$	0.03 to 0.1	–
Lanthanum + lithium	$Ba_{1.8}La_{0.1}Li_{0.1}NaNb_5O_{15}$	0.1	440
Lithium	$Ba_{1.8}Na_{0.9}Li_{0.5}Nb_5O_{15}$	0.5	602
	$Ba_{1.6}Na_{1.4}Li_{0.4}Nb_5O_{15}$	0.4	570
Lead	$Ba_{2(1-x)}Pb_{2-0.5x}Na_{1-0.1x}Nb_5O_{15}$	$0 \leq x \leq 1$	452–497
Potassium	$Ba_2K_xMa_{1-x}Nb_5O_{15}$	<0.5	560–320
Rare earth ions	$Ba_2Na_3RNb_{10}O_{30}$		
	$A_2ReNb_5O_{15}$ (A = alkali metal, Re = Rare earth)		
	$Ba_{1-x}R_{\frac{2x}{3}}Nb_2O_6$		
	$Ba_{4.2x}R_xNb_{10}O_{30}$		
Strontium	$Ba_{2+x-y}Sr_yNa_{1-2x}Nb_5O_{15}$	$0.1 \leq x \leq 0.5$	445–230
Tantalum	$Ba_2NaNb_{5(1-x)}Ta_{5x}O_{15}$	$0.0 \leq x \leq 1.0$	560–(−238)
Titanium	$Ba_{5.3}Na_{0.7}(Nb_{8.7}Ti_{1.3})O_{30}$	1.3	307
Tungsten	$Ba_{2-x}Na_{1+x}Nb_{5-x}W_xO_{15}$	$0 \leq x \leq 1.25$	–

On the basis of X-ray diffraction data Schneck [36, 37] suggested that in rather pure stoichiometric specimen a second IC phase begins at 105 K and terminates at 12 K. This IC phase was supposed to be tetragonal. The presence of such a phase was confirmed by Brillouin studies of acoustic phonon behaviour [38] in BNN above and below its phase transition at 105 K.

In view of the crystal chemistry of BNN, many studies have been carried out to investigate and optimise the outstanding ferroelectric properties of this material by suitable substitutions. These are outlined in Table III.

Ferroelectric curie point found to decrease from 833 K to about 40 K in ceramic $Ba_2NaNb_{5(1-x)}Ta_{5x}O_{15}$ for $x = 0$ to 1. Where as ferroelastic phase transition point from 573 K to 250 K range through dielectric and Raman scattering measurements by Masaaki Takashige *et al*. [39].

Ferroelectric activity in ceramic $Ba_2NaNb_{5(1-x)}Ta_{5x}O_{15}$ was confirmed through the observation of the 50 Hz D-E hysteresis loop for samples with $x \geq 0.4$ by Masaaki Takashige *et al*. [40]. As a result the end member $Ba_2NaTa_5O_{15}$ was assinged a new ferroelectric below the 40 K range.

Effect of non-isoelectronic cation substitution on lattice parameters of BNN was studied by Mukherjee *et al*. [41]. The changes in lattice parameters, a, b and c according to these investigators occurred propotionately for the selective substitution by Gd or Cr. Ravez *et al*. [42] reported that the curie temperature and the permittivity of BNN decrease with increase in Flourine content. Masuda and Wada [43] studied the ferroelectric properties of $La_{0.1}Li_{0.1}NaBa_{1.8}Nb_5O_{15}$. These authors noticed an anomaly in the vicinity of 250°C when La^{3+} ions were substituted for Ba^{2+}, which was not observed in BNN single crystal.

Substitution of lead for alkaline earth element in BNN to yield the solid solution of $Ba_{2(1-x)}Pb_{2.05x}Na_{1-0.1x}Nb_5O_{15}$ for $0 \leq x \leq 1$ was studied by Ravez *et al*. [44]. The T_c and the harmonic efficiency in non linear optics showed a minima for $x = 0.65$. For samples containing $x > 0.65$, partially coupled ferroelectric and ferroelastic properties were simultaneously observed. Substitution of potassium in BNN showed that the advantageous properties of BNN can be retained while eleminating the deleterious effect of micro twinning [45].

The higher symmetry of tetragonal tungsten bronze is obtained at room temperature upon replacing part of Ba ions in BNN with Sr. Substitution of Sr led to the lowering of T_c from 560 to 200°C for Sr content equal to 0.0 to 1.5 in $(Ba_{1-x}Sr_x)_2NaNb_5O_{15}$. The resistivity however increases by two orders of magnitude [46]. The effect of Strontium substitution was also studied by Chen [47] in presence of 0.16% Li_2O and 0.2% MnO_2.

The temperature dependence of the dielectric constant and spontaneous polarisation for the ceramic and polycrystalline samples of mixed system $Ba_2NaNb_{5(1-x)}Ta_{5x}O_{15}$ were investigated over full range of Tantallum concentration, x. It was found that the curie point of BNN lowers from 833 K to about 35 K on substitution of x from 0 to 1 [48, 49].

The orthorhombic to tetragonal transition temperature is lowered [50] with increasing x, when Nb ions in BNN are partially replaced by Ti in the solid solutions of $Ba_{4+x}Na_{2-x}Nb_{10-x}Ti_xO_{30}$.

Altering the Ba, Na, Nb content of compositions near BNN and Sr, Ca, Ta, Li, Na or K substitutions affect T_c and polarisation. For example, as Li concentration in $Ba_{1.8}Na_{0.9}LiNb_5O_{15}$ decreases the T_c is shown to vary from 602 to 570°C. T_c is reported to be primarily dependant upon the Nb/Ba ratio. At room temperature the tetragonal phase is evident for Nb/Ba ≥ 2.8 [21]. Also the presence of tungsten in BNN was found to decrease the distortion of the lattice [51] as well as T_c.

Extensive studies were performed with rare earth substitutions [52–54] in BNN which form a new series of the type $Ba_2Na_3RNb_{10}O_{30}$ where R = La^{3+} Eu^{3+}, Gd^{3+}, Dy^{3+} and Y^{3+}. These materials are solid solutions with TB type structure and exhibit dielectric peaks at temperatures ranging from −25 to 230°C depending on the ionic size of the rare earth ions. The corresponding compositions and their related parameters are shown in Table IV. Another series of the type, $A_2^+Re^{3+}Nb_5O_{15}$ (where Re = La, Sm, Y and A = an alkali) and $[Ba_{1-x}R_{2x/3}]$ Nb_2O_6 (where R = Sm, Y, La) were also studied [55, 56].

TABLE IV Lattice constants, axial ratios and dielectric peak temperatures of the systems $Ba_2Na_3RNb_{10}O_{30}$ and $Ba_3NaRNb_{10}O_{30}$ (after [52–54])

Composition	a	c	$\sqrt{10}\,c/a$	Dielectric-peak temperature (°C)
$Ba_2Na_3LaNb_{10}O_{30}$	12.467	3.914	0.993	−25
$Ba_3NaLaNb_{10}O_{30}$	12.475	3.950	1.001	−50
$BaNa_2La_2Nb_{10}O_{30}$	12.475	3.904	0.990	
$Ba_2Na_3EuNb_{10}O_{30}$	12.429	3.902	0.993	155
$Ba_2Na_3GdNb_{10}O_{30}$	12.417	3.895	0.992	170
$Ba_2Na_3DyNb_{10}O_{30}$	12.405	3.893	0.992	220
$Ba_2Na_3YNb_{10}O_{30}$	12.400	3.900	0.993	220
$Ba_3NaGdNb_{10}O_{30}$	12.449	3.934	0.999	20
$Ba_3NaYNb_{10}O_{30}$	12.423	3.933	1.001	145
$BaNa_2Y_2Nb_{10}O_{30}$	Tungsten-bronze type plus extra phase			

X-ray studies have been made in $Ba_3NaRNb_{10}O_{30}$ (R = La, Sm, Nb and Gd) by Sati *et al.* [57]. The system under study has been found to be tetragonal. Ceramic compositions of $Ba_{4-2x}Na_{2+x}R_XNb_{10}O_{30}$ where $x = 0, 0.3, 0.5$ and 0.7; R = La, Pr, Nd, Sm, Gd, Dy and Y have been studied by Rao and Rao [58, 59]. The ferroelectric curie temperature was found to decrease with the concentration of rare earth ion. The grain size was also reported to decrease with increase of rare earth ion content.

Raman studies by Shawabkh and Scott [60] (of E-Symmetry phonon modes) in BNN (in the tetragonal and above T_c) indicated that the IC-IC transition at 565 K does not alter the orthorhombic symmetry. Also it is not at true, 1q-2q transition and tetragonal symmetry does not set in until the IC normal transition at 582 K. They found IC-IC transition from orthorhombic to tetragonal near 90 K and it is quiet analogous to 565 K. However, electron microscopy showed these phases are not reentrant. The dielectric and brillouin spectroscopy studies [61] on BNN from 15 K to room temperature revealed that 105 K transition is from C_{m2} to a modulated structure, which appears to be a reentrant phase. However neutron diffraction results showed the 2q-1q nature of BNN below ∼100 K.

Thermostimulated erasure of photorefraction (TSEP) [62] is a realiable tool for the trap level investigation, while providing the same information as the other thermostimulated methods, thermostimulated luminescence (TSL) and thermostimulated conductivity (TSC) [63]. As the detected signal in TSEP is monochromatic and well collimated, it can be easily isolated from pyroluminescence and sparking by spatial and frequency filtering. With the use of STEP Gorban *et al.* [64] showed two trap levels in $LiNbO_3$ and ten levels in BNN, photorefractive crystals. Fig. 4. shows the temperature dependence of the diffraction signal intensity for $LiNbO_3$ and BNN crystals obtained from the TSEP technique.

By using growth striation technique, an acoustic super lattice (ASL) of BNN crystals, the single crystals with the periodic laminar ferroelectric domain structure has been prepared by Xu *et al.* [65]. High frequency resonance in the range of 200–400 MZ in BNN has been realised experimentally by the same authors and are in agreement with the prediction of the theory proposed by Zhu [66]. The relationship between resonance frequency, f and periodicity of acoustic super lattice, $a + b$ has been given in Table V. The resonance frequency is 273 MHz closed to theoretical value, 286 MHz which is calculated from the formula [66] $f = v/(a + b)$ with $a + b = 21.5$ μm and $v = 6147$ m/s [67] for resonator No. 3. v and $a + b$ are sound velocity and the periodic length of the ASL respectively. The above experimental results indicate that the application of acoustic devices with low acoustic loss operating at high frequencies is expected.

TABLE V Relationship between the resonance frequency f and periodicity of acoustic superlattice $a + b$ (after [67])

Resonator	Periodicity of superlattice $a + b$ (μm)	Frequency of resonance f (cal.)	(MHz) mes.	Error (%)
No. 1	28.9	213	216	1
No. 2	31.9	193	206	6
No. 3	21.5	286	273	4
No. 4	26.0	236	243	3

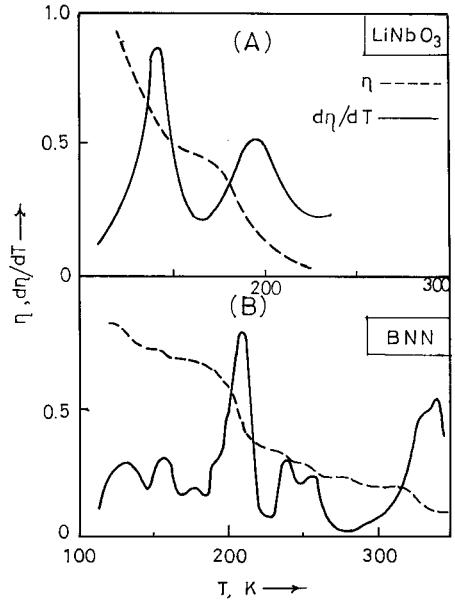

Figure 4 Temperature dependence of diffraction efficiency (dashes) and its temperature derivative (solid lines) for BNN and $LiNbO_3$ (after [64]).

NMR spectra have been measured for the quadrapole perturbed Y2 → Y2 transition of ^{93}Nb in BNN between 300 and 650 K by Nor-Cross *et al.* [68] and found that the spectra are in homogeneously broadened in the IC phase between $T_I = 58$ K and $T_c = 540$ K as well as in the quasi commensurate (Q_C) phase below T_c. However the observed line shapes donot exhibit the characterstic lines for other 1q and 2q modulated incommensurate materials. They explained the temperature dependence of observed line shape using a model in which a phase fluctuation induced by random, weak pinning of modulation wave by defects produced Gaussian line broadening. Further, random pinning of the modulation wave also creates a large phase on gap which makes spin lattice relaxation in a phason's inefficient. They interpreted the results obtained as the presence of defects due to non stoichiometry causes the IC and Qc phases of BNN to be "chaotic".

Both feroelectric and IC transition in $Ba_2NaNb_{5(1-x)}Ta_{5x}O_{15}$ were studied by Mori *et al*. [69] using transition electron microscope to find the relation between these transitions. They found that the ferroelectric transition takes place around 373 K in $x = 0.57$ while IC transition occurs around 543 K. It has been interpreted as the feroelectric transition does not basically accompaning a change in microstructures relative to the IC lattice modulation and further mentioned that there is no interaction between these two transitions.

Temperature dependence of the dielectric constant and spontaneous polarization for the ceramic and polycrystalline compositions of, $Ba_2NaNb_{5(1-x)}Ta_{5x}O_{15}$ were invesigated [70] for $x = 0$ to 1.0. They found that the curie point lowers from 833 K to about 35 K for $x = 0$ to 1.0

Differential scanning calorimetry investigations on single crystal BNN from 400–900 K by Zhu *et al*. [71]. Three thermal peaks were observed; one was at 853 K near FE transition temperature, the two others were at 532 K and 549 K respectively and estimated the corresponding latent heat. They also observed the specific heat anamolae at 590 K. The authors have interpreted these thermal anamolous in the framework of the available structure—transition and IC—phase models.

5. Optical and electro-optic properties

The optical absorption coefficient of single domain BNN was measured over a wave length ranging from 350 nm to approximately 8 μm by Singh *et al*. [72]. The interesting feature of the absorption spectrum of BNN is the presence of a narrow band of half-width 50 cm^{-1} at 3500 cm^{-1}. The same authors also reported a large optical indices of refraction of BNN for various wave lengths by the method of minimum deviation with a wild-Herzburg presission spectrometer. The measured refractive indices of BNN at room temperature are given in Table VI. The measured values of the non-linear coefficients d_{11} and the corresponding coherence lengths for BNN obtained by the same authors have also been shown in Table VII.

The spontaneous polarisation values in $LiNbO_3$, $LiTaO_3$ and BNN have been measured directly at room temperature by a field reversal method for the first time by Wemple *et al*. [29] and found to be P_s ($LiNbO_3$) = 0.71 C/m^2, P_s ($LiTaO_3$) = 0.50 C/m^2 and P_s (BNN) = 0.40 C/m^2. Using these P_s values they showed that the linear electro optic effect in these materials is related fundamentally to a biased quadratic effect associated with each BO_6 octahedron. Based on the above result Wemple *et al*. [29] predicted the spontaneous polarisation in other oxygen octahedra ferroelectrics.

The optical properties of single crystal BNN and barium strontium niobate, typical representatives of oxygen octahedra ferroelectrics were investagated by Mamedov [73] using synchrotron radiation, in the energy range 1.0–35.0 ev. These results were used to calculate the optical function to propose an inter band transition energy scheme (Fig. 5) and to demonstrate the important role of NbO_6 octahedron in the formation of the band structures of the crystals.

Second harmonic generation (SHG) was first demonstrated using a pulsed ruby laser and a quartz crystal [74]. Parametric oscillation (PO) converse effect was subsequently observed using a pulsed $CaWO_4$: Nd laser and a $LiNbO_3$ crystal [75]. $LiNbO_3$ is a ferroelectric material whose useful non-linear coefficient is an order of magnitude larger than that of KDP, one of the best materials previously available. Though the development of YAG : Nd laser facilitated the demonstration of continuous SHG at 0.53 μ using $LiNbO_3$ crystal inside the laser cavity [76, 77], the output power was limited to a few milliwatts due to scattering by refractive index inhomogenities produced in the $LiNbO_3$ crystals by 0.53 μ radiation.

TABLE VI Refractive indices of BNN at room temperature (after [72])

A (nm)	n_x	n_y	n_z
457.9	2.4284	2.4266	2.2931
476.5	2.4094	2.4076	2.2799
488.0	2.3991	2.3974	2.2727
496.5	2.3920	2.3903	2.2678
501.7	2.3879	2.3862	2.2649
514.5	2.3786	2.3767	2.2583
532.1	2.3672	2.3655	2.2502
632.8	2.3222	2.3205	2.2177
1064.2	2.2580	2.2567	2.1700

TABLE VII Non-linear coefficients, coherence lengths, and δ coefficients of BNN at room temperature (after [72])

	$d_{ij}^{a}/d_{11}^{quartz}$ (μm)	i_{ij}^{coh} (obs) (μm)	i_{ij}^{coh} (calc) (μm)	$\delta_{ij}^{a}/\delta_{11}^{quartz}$
d_{21}	40 ± 2	48	33.7	1.48 ± 0.08
d_{22}	40 ± 4	35.9	40.3	1.5 ± 0.1
d_{23}	55 ± 4	3.4	3.32	2.53 ± 0.2
d_{15}	40 ± 2	1.72	1.72	1.46 ± 0.07
d_{24}	38 ± 2	1.72	1.73	1.39 ± 0.07

[a]Barium sodium niobate.

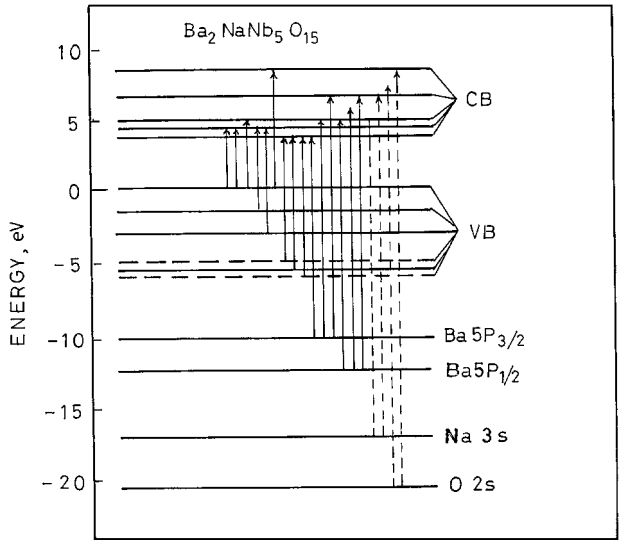

Figure 5 Interband transition scheme in BNN (VB—valence band, CB—conduction band, after [73]).

TABLE VIII A comparision of SHG crystals (after [21])

Property	$Ba_2NaNb_5O_{15}$	$K_3Li_2Nb_5O_{15}$	$LiNbO_3$
Structure	Orthorhombic	Tetragonal	Rhombohedral
Space group	Cmm^2 (C_{2V})	P4bm (C_{4V})	R3 (C_{3V})
Lattice constants in Å units			
a	17.626	12.59	5.14820
b	17.592		
c	3.995	3.97	13.8631
Melting point	1430°C	1050°C	1253°C
Density (in g/cm)	5.4	4.3	4.628
Refractive index at 0.6328 Å			
a	n_x 2.3231	*n* 2.163	*n* 2.00
b	n_y 2.3227	*n* 2.277	*n* 2.286
c	n_z 2.2178		
Curie temperature (T_c)	560°C	420°C	1140°C
Useful nonlinear coefficients:			
d_{31}	35 ± 4	19 ± 4	14.5 ± 2
d_{32}	41 ± 4		
$(1.06 \rightarrow 0.53)^b$	80 and 90°C	80°C	50°C
E (100 kHz) 30°C	47	70	29
V (0.6328)[c]	1400–1500	930	2800
P_S^d	0.40	0.4	0.71
Photoelastic constant P_{31}	0.2		0.2
Acoustic Q (500 MHz, 30°C)	$>1 \times 10$		2×10
Piezoelectric coupling (30°C)	60%		50%

[a]Relative to d_{11} for quartz.
[b]Temperature for phase match without double refraction.
[c]Half-wave retardation voltage for a cube in volts per centimeter
[d]Saturation polarization in coulombs per square meter.

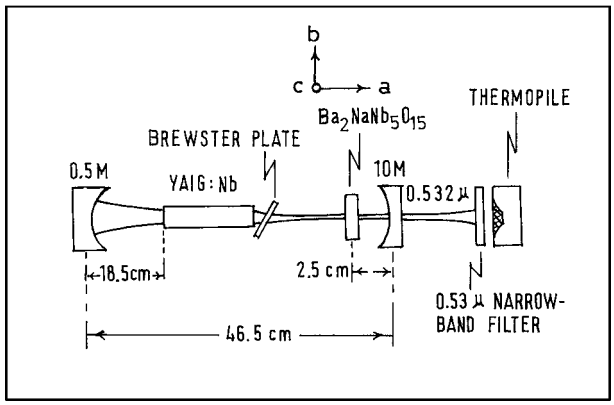

Figure 6 Schematic representation of continuous 0.532 μ solid state source using BNN and YAIG: Nd laser (after [79]).

The useful nonlinear coefficient of BNN is twice that of $LiNbO_3$ and the material does not suffer optical damage for reasonable power levels at room temperature. BNN has been used to obtain 100% convertion of 1.06 μ to 0.53 μ SHG and to demonstrate continuous parametric oscillation [78, 79]. The experimental set up of continuous 0.532 μ solid state using BNN and the YAIG-Nd laser has been shown in Fig. 6. A comparision of SHG parameters of BNN with other materials, $K_3Li_2Nb_5O_{15}$ and $LiNbO_3$ is given in Table VIII [21]. Useful variation of BNN include solid solutions with $LiNbO_3$ or $Na_3Li_2Nb_5O_{15}$, which not only increase Q_T (phase match temperature in °C) but also extends the utility of the material for SHG at wave length less than 1.06 μ. The vacant A sites in Lithium Niobate act as deeper straps where as the vacant A sites in the Niobates with TB like structures act as some what shallower traps. Hence the optical damage suffered by BNN is less than that of $LiNbO_3$. In addition to T_c, P_s and E, the voltage for half wave retardation (V_Π) at 0.6328 μ is 200 V/m in BNN, radiation was studied in Ba, Sr, Na, Niobate series by Van Uitert *et al*. [80]. It is reported that V_Π declines approximately linearly with increasing Sr content but the product $E\ V_\Pi$ tends to remain constant for poled crystals.

Ferroelectric crystals of BNN are used in non-linear optics and in electro-optics. Many ferroelectrics of the oxygen octahedron type exhibit a change in the refractive index under the influence of light (photorefraction) [81, 82] which limits their applications. The photorefractive sensitivity of such crystals varies over wide range. For example, in the case of Fe-doped $LiNbO_3$ crystals the effect is perceptible when the illumination "dose" is 12 mJ/ cm^2 for$\lambda = 488$ nm and the effect is retained for a few months [83]. In the case of BNN crystal, a weak effect is observed only during continuous illumination with a light of 10 watts/cm^2 intensity and $\lambda = 488$ nm and it appears in less than one second after the end of the illumination [84]. Voronov and Yu [85] has performed the physical processes which accompained conversion of BNN crystal to the single domain state as a result of high temperature (630°C, electric field 10–100 Kv/cm) and low temperature (100°C, 3–4 kv/cm) treatment. It has been found that an increase in the electrical conductivity and a charge in the absorption specimen and it is related to the partial loss of oxygen by the crystal and to the Nb^{5+}-Nb^{4+} reduction process. The high temperature treatment gave rise to harmonic oscilations of the voltage across a crystal and the period of these oscilations was a few seconds. The photoconductivity increased stongly in the single-domain state and it decreases slowly photorefraction

under the influence of focused He-Cd laser rediation of approximately 100 w/cm^2 power density demonstrated that the induced change in the birefringence was 7×10^{-6} and it diappears after the end of the illumination. They explained the low photorefractive sensitivity was due to the high photoconductivity.

Singh *et al.* [72] studied the optical absorption, refractive index, non linear optical coefficients and linear electrooptic coefficients for single domain crystals of BNN between room temperature and curie temperature. For 1.064 μm laser fundamental they observed phase match temperature and the angular half width of the phase match second harmonic intensities were found to be in good agreement with the values calculated from refactive index data. The dielectric and electro optic half wave voltage data on BNN according to these authors project BNN to be a useful electro optic modulator material.

Single crystals of $Ba_{5.3}Na_{0.7}Nb_{8.7}Ti_{1.3}O_{30}$ showed several merits in the electro optical applications compared with BNN. An orthorhombic distortion was removed from the crystals unlike BNN which retains it, when the tetragonal–orthorhombic transition point was lowered to -55°C. Better figure of merit was claimed in the above material [50]. The mixed (Pb, Ba, Sr)$_2$ $NaNb_5O_{15}$ crystals show SHG effects that are some what weaker than that for $LiNbO_3$ for 1.062 to 0.53 μ conversion. The efficiency of SHG of BNN compounds in general appear to be comparable to those for the (Pb, Ba, Sr)$_5$ $Nb_{10}O_{30}$ compositions having comparable values of T_c [86].

The ferroelectric axis in BNN crystal has been determined by lvanova *et al.* [87] by observing different patterns of Rayleigh scattering along the *a* and *c* axis. It has been observed that the curie point of BNN by observing abrupt change in the nature of scattering. Also an increase in the angular divergence and a complex angular structure has been observed [88] when a laser light beam passes through BNN crystal, near T_c, at a temperature range 500–560°C.

Scott *et al.* [89] observed that near T_c BNN exhibits a strong thermal focussing of laser light polarised along its optical axis (focal length, $F = +2$ to $+3$ cm for 1 w in a 0.45 mm beam waist). The beam convergence $\theta(T)$ has been found to be proportional to K^{-1} (T) $dn_c(T)/dT$ where K is the thermal conductivity and n_c is the *c*-axis of index of refraction. For zero applied field θ (T) far from T_c is dominated by the isotropic dn/dt, which varies as $t^{2\beta-1}$, where t is reduced temperature and b is the co existence curie exponent. However within a degree or two of T_c, θ (T) is dominated by K (T) which becomes highly anisotropic and has a cusp-like tip for thermal diffusion along polar axis. They observed that a few KV/cm is sufficient to supress the cusp.

The thermal focussing of laser beam in isotropic fluids has been understood in detail for more than 20 years as arising from thermal expansion [90, 91], the decreased density in the laser beam region produces a negative temperature derivative for the index of refraction of order $dn/dT = -1.0 \times 10^{-3}$ K^{-1} and a consequent concave lengths of characterstic focal length, $F = -1.0$ m. A physically different mechanism exists

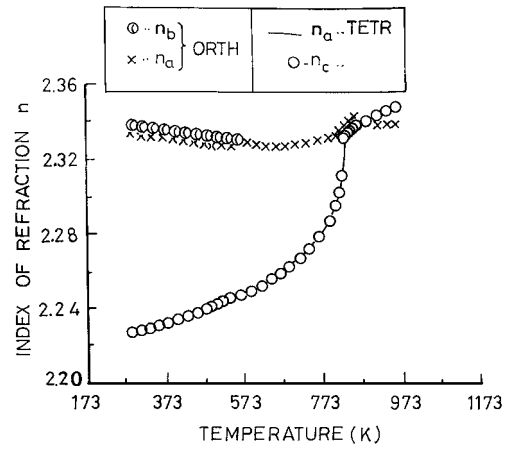

Figure 7 Indices of refraction near T_c in BNN (after [25]).

for even larger values of dn/dT in solids, which may be of either positive or negative sign. BNN examplifies [92] (Fig. 7.) the large changes in indices of refraction and birefringence associated with structural phase transitions in crystals. Here at T_c the value of $dn_c/dt = +1.4 \times 10^{-3}$ K^{-1} produces a convex thermal lens of typical focal length 3 cm. This value is 30 times stronger than isotropic thermal lens effect found in fluids by Gordon *et al.* [90] and of oppostie sign. This effect potentially provides an accurate way of measuring dn/dt very near phase transition temperature which may be useful in studying the critical phenomena associated with structural phase transitions in solids. Also the same authors found that $2\beta = 0.50 \pm 0.05$. Futher temporal effects are found to be in accord with the thermal focusing theories for fluids and yield the thermal diffusivity at T_c.

Using travelling interference pattern and an applied A.C.field Nesterkin *et al.* [93] studied the writing of a static photorefractive grating in BNN crystals. Further they studied two and four wave arrangements by using synchronous-detection technique in the same material. Experimental investigation [94] of the diffraction of the light by ferroelectric domains in BNN crystal revealed that an elastogyration mechanism of the diffraction of light on enantimophic domain existed in BNN crystals.

Based on the studies of the ferroelectric domain structures and the influence of growth striations on para-ferroelectric phase a new type of crystal with periodic or quasi periodic laminar ferro-electric domains of BNN and $LiNbO_3$ have been prepared by Ming [95] and demonstrated that this kind of crystals produces significant effects with regards to optical and accoustical wave process and can be used as a new type of device for a variety of applications in the opto-electronic and accoustoelectric field. Discussion on thermal foccusing in BNN, SBN and PMN materials has been presented by Chen and Scott [96] and emphasised on the determination of critical indices β and δ. Extracting Landau-Devonshire coefficients of frequency expression, quantitative explanation of the temporal and special patterns, critical for optical bi-stability, adiabatic and isothermal responses, and applications to flow-rate and pressure sensors.

Second harmonic generation, microscopic observations has been studied [97] on (001) cut crystal of BNN.

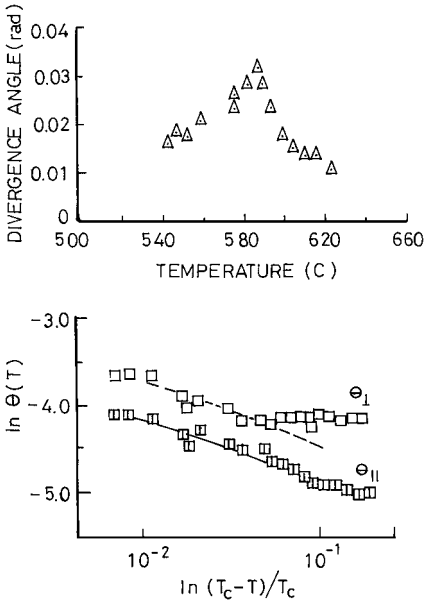

Figure 8 (a, b) Beam divergence θ (T) at study state for 400 mw of 488 nm light along the [100] axes of BNN, with polarisation along [001] as a function of temperature (after [99]).

Microscopic observations revealed that the refractive index fluctuations causes several SHG phase matching conditions. Static photorefractive gratings are recorded by running interference pattern in the BNN crystal with a applied AC field by Nestiorkan *et al*. [98]. The same authors investigated both two and four wave mixing based on the interference pattern.

Scott *et al*. [99] determined the preliminary values of critical exponent β, and found $2\beta = 0.50 \pm 0.05$ in agreement with mean field prediction from the experimental (Fig. 8.) values of beam divergence θ (T) as a function of temperature. They also reported that this unexpected deviation from mean field within ~5 K at T_c. They interpreted this is due to defect mechanism.

The authors [100] have extended the work on thermal focusing near the T_c to include quantitative analysis of external electric field. The results in BNN are consistent with mean field theory near critical point. Also, from the non-zero field theory data the authors were able to extract the Landau coeffients which are more accurate than, but consistent with, estimates based upon previous measurements. These coeffcients gave a model which is weakly first order. Further, application of a 30 Kv/m field drives the model to a critical point. The thermal lens effect is largest at this critical field.

Thermal focussing and optical bistability in BNN, $Sr_{1-x}Ba_xNb_2O_6$ and $PbMg_{1/2}Nb_{2/3}O_3$ near T_c has been described by Chen and Scott [96]. The authors have discussed on (1) determination of critical indices β and δ, (2) extracting Landau-Devonshire coefficients in the free-energy expression, (3) quantitative explanation of temporal and spatial patterns, (4) criteria for optical bistability, (5) adiabatic and isothermal responses, (6) application on flow-rate and pressure sensors. Writing of a static photorefractive grating in the BNN with a travelling interference pattern and an applied alternative field has been studied experimently by Nesterkin *et al*. [101]. Authors have studied the two and four wave arrangements by synchronous-detection method.

Nestiorkin *et al*. [98] have investigated the phase locked detection mechanism using a rapidly running interference pattern and externally applied AC field in BNN crystal. Strong intensification of a photorefractive response compared with that of the traditional diffusion mechanism was observed experimentally for grating periods of 2–100 μm in SBN: Ce crystal. These results confirm the applicability of their method for ferroelectrics. In BNN this technique acts without distruction of the mono domain structure. They examined the contribution of the diffusion mechanism for both two and four wave mixing. Experimental results are reasonably consistent with theory developed [102] previously.

References

1. S. G. ODULOR and O. I. OLEINITH, *Sov. Phys. Solid State* (USA) **17** (1985) 2093.
2. B. BOBBS, M. MATLOUBIAN, H. R. FETTERMAN, R. R. NEURGAONKAR and W. K. CORY, *Proc. SPIE Inst. Soc. Opt. Eng*. (USA) **545** (1985) 35.
3. *Idem*., *Appl. Phys. Lett*. (USA) **48** (1986) 1624.
4. J. E. GEUSIC, H. J. LEVINSTEIN, S. SINGH, R. G. SMITH and L. G. VAN UITERT, *Appl. Phys. Lett*. **12** (1968) 306.
5. R. G. SMITH, J. E. GEUSIC, H. J. LEVINSTEIN, J. J. RUBIN, S. SINGH and L. G. VAN UITERT, *ibid*. **12** (1968) 308.
6. A. MAGNELI and B. BLOMBERG, *Acta. Chem. Scand*. **5** (1951) 372.
7. A. D. WADSLEY, *Rev. Pure Appl. Chem*. **5** (1955) 165.
8. M. H. FRANCOMBE, *Acta. Cryst*. **13** (1960) 131.
9. P. B. JAMIESON, S. C. ABRAHAMS and J. L. BERNSTEIN, *J. Chem. Phys*. **50** (1969) 4353.
10. R. L. BARNS, *J. Appl. Cryst*. **1** (1968) 290.
11. H. IWASAKI, *Mat. Res. Bull*. **6** (1971) 251.
12. Y. ITOH and H. IWASAKI, *ibid*. **7** (1972) 663.
13. B. A. SCOTT, E. A. GIESS and D. F. O'KANE, *ibid*. **4** (1969) 107.
14. J. R. CARRUTHERS and M. GRASSO, *ibid*. **4** (1969) 413.
15. W. A. BONNER, J. R. CARRUTHERS and H. M. O'BRYAN JR., *ibid*. **5** (1970) 243.
16. K. G. BARRACLOUGH, I. R. HARRIS, B. COCKAYNE, J. G. PLANT and A. W. VERE, *J. Mater. Sci*. **5** (1970) 389.
17. J. S. ABELL, K. G, BARRACLOUGH, J. R. HARRIS, A. W. VERE and B. COCKAYANE, *ibid*. **6** (1971) 1084.
18. J. J. RUBIN, L. G. VAN UITERT and H. J. LEVINSTEIN, *J. Cryst. Growth* **1** (1967) 315.
19. A. A. BALLMAN, J. R. CARRUTHERS and H. M. O'BRYAN JR., *ibid*. **6** (1970) 184.
20. A. W. VERE, J. G. PLANT, B. COCKAYNE, K. G. BARRACLOUGH and I. R. HARRIS, *J. Mater. Sci*. **4** (1969) 1075.
21. L. G. VAN UITERT, J. J. RUBIN and W. A. BONNER, IEEE, *J. Quantum Electronics* **4** (1968) 622.
22. J. L. MUKHERJEE, C. P. KHATTAK, K. P. GUPTA and F. F. Y. WANG, *J. Solid State Chem*. **24** (1978) 163.
23. Y. TANOKURA, M. TSUKIOKA, M. KOBAYASHI and S. TSUMI, *Mod. Phys. Lett*. B (Singapore) **4** (1990) 1053.
24. J. BURGEAT and J. C. TOLEDANO, *Solid State Comm*. **20** (1976) 281.
25. T. YAMADA, H. IWASAKI and N. NIIZAKI, *J. Appl. Phys*. **41** (1970) 4141.
26. TAKURO IKEDA, *Jap. J. Appl. Phys*. **13** (1974) 1065.
27. T. L. REINECKE and K. L. NAGI, *Ferroelectrics* **20** (1978) 309.
28. J. C. TOLEDANO, *Phys. Rev*. B **12** (1975) 943.
29. S. H. WEMPLE, M. DIDOMENICO JR. and I. CAMLIBEL, *Appl. Phys. Lett*. **12** (1968) 209.
30. A. W. WARNER, G. A. COQUIN and J. L. FINK, *J. Appl. Phys*. **40** (1969) 4353.
31. A. V. TURIK, E. N. SUDERINKO and V. G. KRYSHTOP, *Sov. Phys. Solid State* **25** (1983) 1177.

32. W. F. OLIVER, Ph.D Thesis University of Colorado (1988).
33. W. F. OLIVER III and J. F. SCOTT, *Ferroelectrics* **117** (1991) 63.
34. G. BURNS and D. F. O'KANE, *Phys. Lett.* **28A** (1969) 776.
35. J. S. ABELL, I. R. HARRIS and B. COCKAYNE, *J. Mater. Sci.* **8** (1973) 667.
36. J. SCHNECK and D. PAQUET, *Ferroelectrics* **21** (1978) 577.
37. J. SCHNECK, J. PRIMOT, R. VANDER MUHLL and J. RAVEZ, *Solid State Comm.* **21** (1997) 57.
38. M. ZHANG, J. YAGI, W. F. OLIVER and J. F. SCOTT, *Phys. Rev.* B **33** (1986) 1381.
39. M. TAKASHIGE, S. KOJIMA, S.-I. HAMAZAKI, F. SHIMIZU and M. TSUKIOKA, *Jpn. J. Appl. Phys.* **32** (1993) 4384.
40. M. TAKASHIGE, S.-I. HAMAZAKI, M. TSUKIOKA, F. SHIMIZU, H. SUZUKI and S. SAWADA, *J. Phy. Soc. Japan* **62** (1993) 1486.
41. J. L. MUKHERJEE, C. P. KHATTAK, K. P. GUPTA and F. F. Y. WANG, *J. Mater. Sci* **13** (1978) 851.
42. J. RAVEZ, B. ELOUAD and P. HAGENMULLER, *Ferroelectrics* **21** (1978) 583.
43. Y. MASUDA and M. WADA, *ibid.* **8** (1974) 515.
44. M. J. RAVEZ, A. PERRON-SIMON, B. ELOUADI, L. RIVOALLAN and P. HAGENMULLER, *J. Chem. Solids* **37** (1976) 949.
45. G. BURNS, *IEEE Transactions on Electron Devices* **16** (1969) 506.
46. L. G. VAN UITERT, J. J. RUBIN, W. H. GRODKIEWIEZ and W. A. BONNER, *Mat. Res. Bull* **4** (1969) 63.
47. T. J. CHEN, O. K. CHON and Y. GNO, *J. Chinese Silicate Soc.* **6** (1978) 32.
48. M. POUCNARD, J. P. CHAMINADE, A. PERRON, J. RAVEZ and P. HAGENMULLER, *J. Solid State Chem.* **14** (1970) 274.
49. M. TAKASHIGE, S. HAMAZAKI, M. TSUKIOKA, F. SHIMIZU, H. SUZUKI and S. SAWADA, *J. Phy. Soc. Jpn.* **62** (1993) 1486.
50. T. IKEDA and JUN-ICHKATA, *Jap. J. Appl. Phys.* **13** (1974) 1792.
51. J. M. REAU, B. ELOUADI, J. RAVEZ and E. T. PAUL HAGENMULLER, *J. Solid State Chem.* **15** (1975) 18.
52. H. IWASAKI, *Mat. Res. Bull.* **6** (1971) 53.
53. H. IWASAKI and S. MIYAZAWA, *Jpn. J. Appl. Phys.* **10** (1971) 161.
54. K. S. SINGH, R. SATI, R. N. PCHOUDARY and K. L. YADAV, in Proc. Vth Nat. Seminar on Ferroelectrics and Dielectrics (India), 1990, p. 95.
55. B. A. SCOTT, E. A. GEISS, G. BURNS and D. F. O'KANE, *Mat. Res. Bull.* **3** (1968) 831.
56. K. MASUNO, *J. Phys. Soc. Japan* **19** (1964) 323.
57. R. SATI, K. S. SINGH, R. N. P. CHOUDARY and K. L. YADAV, in Proc. VI th Nat. Seminar on Ferroelectrics and Dielectrics (India) 1990, p. 138.
58. P. S. V. SUBBA RAO and K. SAMBASIVA RAO, *Ferroelectrics* **67** (1986) 167.
59. P. S. V. SUBBA RAO, K. SAMBASIVA RAO and A. BHANUMATI, *J. Mater. Sci. Lett.* **6** (1987) 299.
60. A. SHAWABKEH and J. F. SCOTT, *Phys. Rev. B: Conds. Matter (USA)* **43** (1991) 1099.
61. WILLIAM F. OLIVER III and J. F. SCOTT, *Ferroelectrics* **117** (1991) 63.
62. Z. MALEK, F. MORAVEC, J. STRAJBLOVA and J. NOVOTNY, *J. Phys. Soc. Jpn.* B (Suppl.) (1969) 430.
63. J. STANKOWASKA and E. CZOSNOWSKA, *Acta Phys. Polon* A **43** (1973) 641.
64. I. GORBAN, S. ODOULOV, O. OLEINIK and M. SOSKIN, *Ferroelectrics* **117** (1991) 83.
65. HIN-PING XU, GVO-ZHONG JIANG, LUN MAO, YOUNG-YUAN, ZHU, MING-QI, NAIBEN MING, JIAN-HUAYIN and YONG-ANSHNI, *J. Appl. Phys.* **71** (1992) 2480.
66. Y. Y. ZHU, N. B. MING, W. H. JIANG and Y. A. SHUI, *Appl. Phys. Lett.* **53** (1988) 2278.
67. A. W. WARNER, G. A. COQUIN and J. L. FINK, *J. Appl. Phys.* **40** (1969) 4353.
68. J. A. NORCROSS, D. C. AILION, R. BLERIC, D. DOHINSEK, T. APIH and J. SLAK, *Phys. Rev. B. Conds. Matt. (USA)* **50** (1994) 3625.
69. S. MORIE, N. YAMANOTO, N. KOYAMAY, HAMAZAKIS and ZAKASHIGE, *ibid.* **52** (1995) 9117.
70. MASAAKI TAKASHIGE, SIN-ICHIHAMAZAKI, MASAYUKI TSUKIOKA, FUMINAO SHIMIZU, HARUHIKO SUZUKI and SHOZO SAWADA, *Ferroelectrics* **158** (1994) 187.
71. SHINING ZHU, NIABEN MING and QINGPING DAI, *Phy. Rev* B **47** (1993) 15280.
72. S. SINGH, D. A. DRAEGERT and J. E. GENSIC, *ibid.* **2** (1970) 2709.
73. A. MAMEDOV, *Sov. Phys. JEPT* **56** (1982) 1043.
74. P. A. FRANKEN, E. A. HILL, C. W. PETERS and G. WEINREICH, *Phys. Rev. Lett.* **7** (1961) 118.
75. J. A. GIORDA MAINE and R. C. MILLER, *ibid.* **14** (1965) 973.
76. J. E. GENSIC, H. M. MARCOS and L. G. VAN UITERT, *Appl. Phys. Lett.* **4** (1964) 182.
77. R. G. SMITH, K. NASSAN and M. F. GALVIN, *ibid.* **7** (1965) 256.
78. L. G. VAN UITERT, S. SINGH, H. J. LEVINSTEIN, J. E. GENSIC and W. A. BONNER, *ibid.* **11** (1967) 269.
79. J. E. GENSIC, H. J. LEVINSTEIN, S. SINGH, R. G. SMITH and L. G. VAN UITERT, *ibid.* **12** (1968) 306.
80. L. G. VAN UITERT, H. J. LEVINSTEIN, J. J. RUBIN, C. D. CAPIO, E. F. DEARBORNAND and W. A. BONNER, *Mat. Res. Bull.* **3** (1968) 47.
81. D. VONDER LINDE and A. M. GLASS, *Appl. Phys.* **8** (1975) 85.
82. V. V. VOROMOV, YU. S. KUZMIVOV and V. V. OSLKO, *Kvanlovaya Ellektton (Moscow)* **3** (1976) 2101.
83. D. L. STACBLER and W. PHILLIPS, *Appl. Opt.* **13** (1974) 78.
84. J. J. AMODEL, D. L. STACBLER and A. W. STEPHENS, *Appl. Phys. Letts.* **18** (1971) 507.
85. V. V. VOROMOV and YU. S. KUZMIVOV, *Sov. Phys. Solid State* **20** (1978) 224.
86. P. V. LENGO, E. G. SPENCER and A. A. BALLMAN, *APPl. Phys. Lett.* **11** (1967) 23.
87. S. V. IVANOVA, I. I. NAUMORA and T. T. SULTA NOV, *Sov. Phy.-Lebedev. Inst. Rep. (USA)* **7** (1989) 52.
88. *Idem.*, *ibid.* **9** (1989) 64.
89. J. F. SCOTT, SHOU-JANG SHEIH, *J. Phys. Cond. Matt. UK.* **2** (1990) 855.
90. P. GORDON, R. C. C LEITE, R. S. MOORE, S. P. S. PORTO and J. R. WHINNERY, *J. Appl Phys.* **36** (1965) 3.
91. CHEMMING HU and J. R. WHINNERY, *Appl. Opt.* **12** (1973) 72.
92. J. F. SCOTT, SHOU-LONG SHEIH, K. R. FURER and N. A. CLARK, W. F. OLIVER and S. A. LEE, *Phys. Rev.* B **41** (1990) 9330.
93. O. R. NESLERKIN, E. P. SHESSHAKOV, B. YAZELDO VICH and A. D. NOVIKOR, *JETP Lett.* (USA) **56** (1992) 299.
94. R. O. VLOKH and I. P. SKAB, *Sov. Phys. Solid State (USA)* **34** (1992) 1739.
95. N. B. MING, *Ferroelectrics* **142** (1992) 35.
96. TING CHEN and J. F. SCOTT, *ibid.* **143** (1993) 149.
97. M. TSUKIOKE, T. FURIMOTO and S. TSUTSUMI, *Mod. Phy. Lett.* B. **8** (1994) 785.
98. O. P. NESTIORKAN, YE. P. SHERSHAKOV, B. YA. ZELDOVICH and A. D. NOVILOV, *Opt. Lett. (USA)* **18** (1993) 684.
99. *Idem.*, *ibid.* **18** (1993) 684.
100. SHOU-JONG SHEIH, P. D. BEALE, TING CHEN and J. F. SCOTT, *Ferroelectric* **123** (1991) 1.
101. O. R. NESTREKIN, E. P. SHERSHAKOV and B. YA. ZEL'DOVICH and A. D. NOVIKOV, *JETP Lett.***56** (1996) 299.
102. P. N. LINKYKH, O. P. NESTIORKIN and B. YA. ZEL'DOVICH, *J. Opt. Soc. Amer.* B **8** (1991) 1042.

Received 20 February
and accepted 23 May 2002